Asymptotic Reference Tracking and Disturbance Rejection of UDE-Based Robust Control

Beibei Ren, *Member, IEEE*, Qing-Chang Zhong, *Fellow, IEEE*, and Jiguo Dai, *Student Member, IEEE*

***Abstract*—The uncertainty and disturbance estimation (UDE)-based robust control strategy is able to achieve good robust performance by estimating and compensating the uncertainty and disturbance in a system with a filter having the appropriate frequency characteristics. However, how to systematically design the filter and the reference system in a UDE-based control system to achieve asymptotic reference tracking and disturbance rejection is still missing in the literature. In this paper, this is solved by applying the well-known internal model principle. The conditions to guarantee the closed-loop system stability and to achieve asymptotic disturbance rejection and reference tracking are derived. Experimental results on a servo system are presented as an example to demonstrate its excellent performance, which can actually reach the hardware resolution limit, with comparisons to the disturbance-observer-based control and the active disturbance rejection control.**

***Index Terms*—Asymptotic disturbance rejection, asymptotic tracking, internal model principle, robust control, uncertainty and disturbance estimator (UDE).**

I. INTRODUCTION

MANY systems have unknown dynamics, modeling errors, various sorts of disturbances, and noise. When the uncertainty/disturbance is measurable, the measured information can be feedfowarded to compensate its effects before it affects the system. Otherwise, several other strategies are available. For example, the adaptive control is capable of handling parametric uncertainties by adjusting the control parameters [1] and the adaptive neural network control works for nonparametric uncertainties, e.g., unmodeled dynamics, by identifying it on the basis of the universal function approximation theorem within a compact set [2]–[4]. With the robust control framework, a nominal model of the plant is assumed, and a controller is sought such that the closed-loop performance and stability are guaranteed for all plant perturbations not greater than a prespecified bound [5]. The sliding-mode control is another robust

control method for uncertain systems, where the uncertainty is handled by the high-gain feedback in order to guarantee the accessibility of the sliding mode [6]–[8].

Another class of approaches lies in the direct extraction of the uncertainty and disturbance information from the system dynamics and input signal. The disturbance observer (DOB)-based control estimates the uncertainty and disturbance by using the inverse of the nominal plant model and a Q-filter [9]–[12]. The DOB-based control is applicable for stable, unstable, minimum phase, and nonminimum phase systems with different bandwidth constraints [13]. The active disturbance rejection control (ADRC) method treats the total disturbance including both the uncertainty and disturbance as an additional state and estimates it via an extended state observer (ESO) [14]–[18]. The equivalent-input-disturbance approach [19] interprets the uncertainty and disturbance as being applied at the input and then estimates it. The time delay control [20] uses the past observation of uncertainty and disturbance as the estimation to modify the control action directly, based on the assumption that a continuous signal remains unchanged during a small enough period (delay). The uncertainty and disturbance estimator (UDE)-based control [21] follows this idea, but employs a low-pass filter instead of a delay term.

In the UDE-based control design, the filter plays a very important role in estimating the uncertainty and disturbance. One option is to choose it as a strictly proper stable filter with unity gain and zero phase shift over the spectrum of the uncertainty and disturbance [21]–[23]. In practice, a low-pass filter is often enough to serve the purpose [21]. In [22], the two-degree-of-freedom nature of the UDE-based control has been revealed, which enables the decoupled design of the reference model and the filter. Some methods have been proposed for the filter design, e.g., in [24]–[27]. However, how to systematically design the filter to achieve asymptotic disturbance rejection in general is still missing in the literature. Another aspect that is not exposed fully is that the UDE-based control is formulated in a way for the system state to track the reference state. Hence, the system state is able to asymptotically track the reference state but not the reference. In other words, there may be a gap between the desired reference signal and the system state. In this paper, these two problems will be addressed thoroughly, based on the well-known internal model principle [28]–[31], and systematic design guidelines for the filter and the reference system will be provided. Then, the conditions to guarantee the closed-loop system stability and to achieve the asymptotic disturbance rejection and reference tracking will be derived. Extensive

experimental results on a servo system are presented as an example to validate the systematic design procedure with comparison to the DOB-based controller designed with the internal model principle and a third-order ADRC. Following the systematic approach proposed in this paper, the performance of the UDE-based controller is better than that of the other two methods and can reach the hardware resolution limit. The results in this paper may provide some insights to further improve the other controllers.

II. PRELIMINARIES AND PROBLEM FORMULATION

A. Overview of the UDE-Based Control Strategy

The UDE-based control framework is applicable to nonlinear or linear, time-varying, or time-invariant systems. In order to facilitate the presentation, consider the following uncertain linear time-invariant system:

$$\dot{x}(t) = (A + \Delta A)x(t) + Bu(t) + d(t) \quad (1)$$

where $x(t) = [x_1(t), \ldots, x_n(t)]^T \in R^n$ is the state, $u(t) \in R$ is the control input, $A \in R^{n \times n}$ is the known state matrix, $\Delta A \in R^{n \times n}$ is the unknown state matrix, $B \in R^n$ is the control vector, and $d(t) \in R^n$ is the external disturbance. The UDE-based control adopts a stable reference model to meet the desired specifications of the closed-loop control system, e.g., overshoot and settling time. Assume the reference model is

$$\dot{x}_m(t) = A_m x_m(t) + B_m c(t) \quad (2)$$

where $x_m(t) \in R^n$ is the reference state vector, and $c(t) \in R$ is a piecewise continuous and uniformly bounded command to the reference model.

The objective is to design a control law $u(t)$ such that $x(t)$ asymptotically tracks the reference state $x_m(t)$ and, ideally, the tracking error $e(t) = x_m(t) - x(t)$ satisfies the dynamics

$$\dot{e}(t) = (A_m + K)e(t) \quad (3)$$

where $K \in R^{n \times n}$ is an error feedback gain matrix and $A_m + K$ is Hurwitz.

Combining (1)–(3) results in

$$A_m x(t) + B_m c(t) - Ax(t) - \Delta Ax(t)$$
$$\qquad - Bu(t) - d(t) = Ke(t). \quad (4)$$

Then, the control action $u(t)$ should satisfy

$$Bu(t) = A_m x(t) + B_m c(t) - Ax(t) - u_d - Ke(t) \quad (5)$$

where

$$u_d = \Delta Ax(t) + d(t) \quad (6)$$

denotes the unknown terms in (4), including the uncertainty term ΔAx and the external disturbance term $d(t)$. Based on (5), the control law $u(t)$ is designed as

$$u(t) = B^+(A_m x(t) + B_m c(t) - Ax(t) - u_d - Ke(t)) \quad (7)$$

where $B^+ = (B^T B)^{-1} B^T$ is the pseudoinverse of B. This is the accurate solution of (5) if the following structural constraint

is met:

$$(I - BB^+) \cdot (A_m x(t) + B_m c(t) - Ax(t) - u_d - Ke(t)) = 0. \quad (8)$$

Otherwise, it is the least-squares approximate solution of (5). According to the system dynamics described by (1), u_d can be represented as

$$u_d = \Delta Ax(t) + d(t) = \dot{x}(t) - Ax(t) - Bu(t). \quad (9)$$

Following the procedures in [21], it can be approximated by

$$\hat{u}_d = u_d * g_f(t) = (\dot{x}(t) - Ax(t) - Bu(t)) * g_f(t) \quad (10)$$

where "$*$" is the convolution operator and $g_f(t)$ is the impulse response of a strictly proper stable filter $G_f(s)$ with the appropriate frequency characteristics, e.g., having unity gain and zero phase shift, over the spectrum of u_d. Replacing u_d with $\hat{u}_d$ in (7), the UDE-based control law is formulated as

$$u(t) = B^+ \left[-Ax(t) + \mathcal{L}^{-1}\left\{ \frac{1}{1 - G_f(s)} \right\} * (A_m x(t) \right.$$
$$\left. + B_m c(t) - Ke(t)) - \mathcal{L}^{-1}\left\{ \frac{sG_f(s)}{1 - G_f(s)} \right\} * x(t) \right] \quad (11)$$

where $\mathcal{L}^{-1}\{\cdot\}$ is the inverse Laplace transform operator.

B. Two-Degree-of-Freedom Nature of the UDE-Based Control

As shown in (11), the UDE-based controller includes three design parameters: a reference model, an error feedback gain, and a filter. After taking the Laplace transform for (1)–(3) and making some manipulations as detailed in [22], it can be shown that, when the structural constraint (8) is met, there is[1]

$$X(s) = H_m(s)C(s) + H_d(s)BB^+ U_d(s) \quad (12)$$

where

$$H_m(s) = (sI - A_m)^{-1} B_m \quad (13)$$

is the transfer function matrix of the reference model given in (2) from $C(s)$ to $X_m(s)$, which is independent of K, and

$$H_d(s) = H_f(s)H_k(s) \quad (14)$$

with

$$H_f(s) = 1 - G_f(s) \quad (15)$$
$$H_k(s) = (sI - (A_m + K))^{-1}. \quad (16)$$

Hence, the UDE-based control inherently has a two-degree-of-freedom structure, i.e., the set-point response is determined by the reference model and the disturbance response is determined by the error feedback gain and the filter, which allows decoupling between reference tracking and disturbance rejection. Moreover, the design of the error feedback gain and the filter is decoupled in the frequency domain [22].

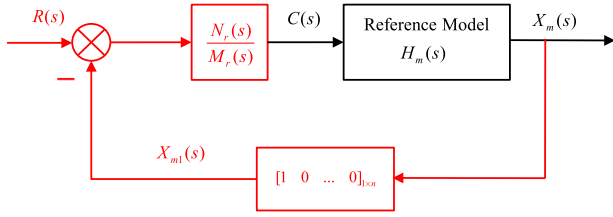[1]Note that there is a typo in [22], where BB^+ in (12) is missing.

Fig. 1. Reference system to achieve asymptotic tracking.

C. Problem Formulation

Although the reference model $H_m(s)$ (2) or (13) is chosen to meet the performance of the closed-loop system, e.g., overshoot and settling time, it may not be able to guarantee asymptotic reference tracking. Moreover, how to design the filter to achieve asymptotic disturbance rejection is not clear. The problem to be solved in this paper is formulated as follows: How to design a filter $G_f(s)$ in the UDE-based controller and a reference system to generate the command $c(t)$ for the reference model $H_m(s)$ so that the system output $y(t) = x_1(t)$ asymptotically tracks the desired reference $r(t) \in R$ and rejects the disturbance $d(t)$, i.e.,

$$\lim_{t \to \infty}(y(t) - r(t)) = 0.$$

III. DESIGN OF THE REFERENCE SYSTEM

In order to simplify the exposition in the following, it is assumed that it is required for $x_{m1}(t)$ to asymptotically track the reference signal $r(t)$. The well-known internal model principle [28] says that, when tracking a reference trajectory or rejecting a disturbance, the asymptotic reference tracking/disturbance rejection can be achieved if the feedback mechanism incorporates a device (the exosystem) that is able to generate the reference trajectory or the disturbance. In order to achieve this, the control strategy shown in Fig. 1 is proposed to generate the command $c(t)$ to the chosen reference model $H_m(s)$ so that $x_{m1}(t) \to r(t)$ when $t \to \infty$, where two more components are added to modify the conventional UDE design in Section II-A.

Assume that the reference trajectory $r(t)$ in Fig. 1 is driven by the following exosystem:

$$\dot{w}_r(t) = S_r w_r(t)$$
$$r(t) = P_r w_r(t) \tag{17}$$

where $w_r(t)$ is the state of the reference exosystem, and S_r and P_r are matrices determined by the characteristics of $r(t)$. Then, $M_r(s)$ in Fig. 1 can be chosen as the characteristic function of the matrix S_r, i.e.,

$$M_r(s) = |sI - S_r| \tag{18}$$

and $N_r(s)$ can be designed as a polynomial or a rational function to stabilize the loop and make $\frac{N_r(s)}{M_r(s)}$ proper. The closed-loop transfer function from $R(s)$ to $X_{m1}(s)$ in Fig. 1 can then be obtained as

$$\frac{X_{m1}(s)}{R(s)} = \frac{N_r(s)H_{m1}(s)}{M_r(s) + N_r(s)H_{m1}(s)} \tag{19}$$

where $H_{m1}(s) = [1, 0, \ldots, 0]_{1 \times n} H_m(s)$. For the choice of $M_r(s)$ in (18), the steady-state gain of (19) is equal to 1 because $M_r(s) = 0$ at the modes of the reference signal $r(t)$, which guarantees the asymptotic reference tracking of $x_{m1}(t)$ to $r(t)$ when $t \to \infty$. Two special cases are given below.

A. Tracking a Step Signal

If the reference signal is a step signal, then $S_r = 0$. According to (18)

$$M_r(s) = |sI - S_r| = s. \tag{20}$$

$N_r(s)$ can be chosen as

$$N_r(s) = k$$

with $k > 0$. Because the reference model $H_m(s)$ is chosen stable, the parameter k can be easily determined, e.g., by using the root-locus approach. Note that, for a stable reference model $H_m(s)$, it is always possible to choose $N_r(s) = k_1 s + k_2$ with $k_1 \geq 0$, $k_2 > 0$ to stabilize the closed loop of the reference system in Fig. 1. Substituting (20) into (19) results in

$$\frac{X_{m1}(s)}{R(s)} = \frac{N_r(s)H_{m1}(s)}{s + N_r(s)H_{m1}(s)}.$$

At $s = 0$

$$\frac{X_{m1}(0)}{R(0)} = \frac{N_r(0)H_{m1}(0)}{N_r(0)H_{m1}(0)} = 1$$

which guarantees the asymptotic tracking of a step signal.

B. Tracking a Sinusoidal Signal

For a sinusoidal reference signal with the known frequency ω_0 (the amplitude information is not required), $S_r = \begin{bmatrix} 0 & \omega_0 \\ -\omega_0 & 0 \end{bmatrix}$. Then, according to (18)

$$M_r(s) = |sI - S_r| = \begin{vmatrix} s & -\omega_0 \\ \omega_0 & s \end{vmatrix} = s^2 + \omega_0^2. \tag{21}$$

$N_r(s)$ can be chosen as

$$N_r(s) = k_1 s + k_2$$

with k_1, $k_2 > 0$ to stabilize the closed loop of the reference system in Fig. 1. At the frequency ω_0, with the choice of M_r in (21), the gain of (19) is calculated as

$$\frac{X_{m1}(j\omega_0)}{R(j\omega_0)} = \frac{N_r(j\omega_0)H_{m1}(j\omega_0)}{N_r(j\omega_0)H_{m1}(j\omega_0)} = 1.$$

It guarantees the asymptotic tracking of a sinusoidal signal at the known frequency ω_0.

IV. DESIGN OF THE FILTER

In this section, the filter will be designed based on the internal model principle to achieve asymptotic disturbance rejection. Assume that the disturbance $d(t)$ in (1) is driven by the following exosystem:

$$\dot{w}_d(t) = S_d w_d(t)$$
$$d(t) = P_d w_d(t) \tag{22}$$

where $w_d(t)$ is the state of the disturbance exosystem, and S_d and P_d are matrices determined by the characteristics of $d(t)$. Due to the definition of the uncertainty and disturbance term u_d in (6), both the disturbance exosystem S_d and the reference exosystem S_r should be included in the filter H_d in (12) in order to achieve asymptotic disturbance rejection. Define $M_d(s)$ as the least common multiple (lcm) of the characteristic functions of S_d and S_r, i.e.,

$$M_d(s) = lcm(|sI - S_d|, |sI - S_r|). \qquad (23)$$

Since $H_k(s)$ and $H_f(s)$ are decoupled in the frequency domain, the filter G_f can be designed so that $H_f(s) = 1 - G_f(s)$ incorporates both the disturbance exosystem S_d and the reference exosystem S_r in the following way:

$$H_f(s) = 1 - G_f(s) = \frac{M_d(s)}{N_d(s)}$$

where $N_d(s)$ can be designed as a polynomial or a rational function, with $\frac{M_d(\infty)}{N_d(\infty)}$ being a finite value, so that no modes of the exosystems can pass H_f. This leads to the

$$G_f(s) = 1 - \frac{M_d(s)}{N_d(s)} \qquad (24)$$

which is proper and hence implementable. Note that $N_d(s)$ should be stable. Three special cases are shown below.

A. With $M_d(s) = s$

This happens when both of the disturbance $d(t)$ and the reference signal $r(t)$ are step signals, i.e., $S_d = S_r = 0$. According to (23)

$$M_d(s) = lcm(|sI - S_d|, |sI - S_r|) = s.$$

If $N_d(s)$ is chosen as a polynomial

$$N_d(s) = s + a$$

with $a > 0$, then the UDE filter can be calculated as

$$G_{f1}(s) = 1 - \frac{M_d(s)}{N_d(s)} = \frac{a}{s + a}.$$

This is actually the low-pass filter frequently adopted in the UDE-based control [21]. Note that the steady-state gain of $G_{f1}(s)$ is 1, and it guarantees the asymptotic tracking and disturbance rejection for step references and disturbances. Other choices of $N_d(s)$ are possible, e.g., to obtain the α-filter $G_f(s) = \frac{(1-\alpha)\tau s + 1}{\tau s + 1}$, as suggested in [26].

B. With $M_d(s) = s^2 + \omega_0^2$

In this case, both the disturbance $d(t)$ and the reference signal $r(t)$ are sinusoidal signals with the known frequency ω_0, i.e., $S_d = S_r = \begin{bmatrix} 0 & \omega_0 \\ -\omega_0 & 0 \end{bmatrix}$. According to (23)

$$M_d(s) = lcm(|sI - S_d|, |sI - S_r|)$$
$$= \begin{vmatrix} s & -\omega_0 \\ \omega_0 & s \end{vmatrix} = s^2 + \omega_0^2.$$

If $N_d(s)$ is chosen as a polynomial

$$N_d(s) = s^2 + a_1 s + a_2$$

then

$$G_{f2}(s) = 1 - \frac{M_d(s)}{N_d(s)} = 1 - \frac{s^2 + \omega_0^2}{s^2 + a_1 s + a_2}$$
$$= \frac{a_1 s + a_2 - \omega_0^2}{s^2 + a_1 s + a_2}.$$

Its gain is equal to 1 at the frequency ω_0, which guarantees the asymptotic reference tracking and disturbance rejection for sinusoidal reference and disturbance signals with the known frequency ω_0. Note that the amplitude of the signal is not required. Only the frequency of the signal is required for the filter design, which is often available or can be identified in most cases based on the characteristics of the system or through some frequency identification approaches [30].

C. With $M_d(s) = s(s^2 + \omega_0^2)$

This happens when one of the reference signal $r(t)$ and the disturbance $d(t)$ is a step signal and the other is a sinusoidal signal with frequency ω_0. Following the previous procedure, it can be obtained that

$$M_d(s) = lcm(s, \ s^2 + \omega_0^2) = s(s^2 + \omega_0^2).$$

If $N_d(s)$ is chosen as a polynomial

$$N_d(s) = (s + a)(s^2 + a_1 s + a_2)$$

then

$$G_{f3}(s) = 1 - \frac{M_d(s)}{N_d(s)} = \frac{(a + a_1)s^2 + (a_2 + aa_1 - \omega_0^2)s + aa_2}{(s + a)(s^2 + a_1 s + a_2)}.$$

Its gain is equal to 1 at both the frequency 0 and the frequency ω_0, which guarantees the asymptotic disturbance rejection.

V. ANALYSIS OF CLOSED-LOOP STABILITY AND ASYMPTOTIC PERFORMANCE

By integrating both designs of the reference system in Section III and the filter in Section IV into the UDE design in Section II, the closed-loop system with the detailed UDE-based robust control is presented in Fig. 2. For the stability analysis, the measurement noise $N(s)$ is assumed to be negligible. The impact of the measurement noise will be investigated in Section V-C. According to Fig. 2, there are

$$sX(s) = (A + \Delta A)X(s) + D(s) + BB^+ U'(s) \qquad (25)$$

$$U'(s) = B_m C(s) + (A_m - A)X(s) - KE(s)$$
$$- G_f(s)(sX(s) - AX(s) - BB^+ U'(s)) \qquad (26)$$

from which it can be found that

$$U'(s) = B_m C(s) + (A_m - A)X(s) - KE(s)$$
$$- G_f(s)U_d(s) \qquad (27)$$

where

$$U_d(s) = \Delta A X(s) + D(s) \qquad (28)$$

Fig. 2.   UDE-based closed-loop system for asymptotic tracking and disturbance rejection.

is the Laplace transform of the lumped term u_d of uncertainty and disturbance. Substituting (27) and (28) into (25), we obtain

$$sX(s) = AX(s) + U_d(s) + BB^+(B_m C(s)$$
$$+(A_m - A)X(s) - KE(s) - G_f(s)U_d(s)). \quad (29)$$

Since $X(s) = X_m(s) - E(s)$ and $sX_m(s) = A_m X_m(s) + B_m C(s)$, then the actual error dynamics is

$$sE(s) = (A_m + K)E(s) - BB^+[1 - G_f(s)]U_d(s)$$
$$+(I - BB^+)(A_m X(s) + B_m C(s) - AX(s)$$
$$-U_d(s) - KE(s)). \quad (30)$$

With $E(s) = X_m(s) - X(s)$, $sX_m(s) = A_m X_m(s) + B_m C(s)$, and $U_d(s) = \Delta AX(s) + D(s)$, the closed-loop system dynamics can be obtained from (30) as

$$[sI - (A_m + K) - BB^+(1 - G_f(s))\Delta A$$
$$+ (I - BB^+)(A_m + K - A - \Delta A)]X(s) = BB^+(B_m C(s)$$
$$- KX_m(s)) + (I - BB^+ G_f(s))D(s). \quad (31)$$

A. Stability of the Closed-Loop System

Theorem 1: The closed-loop system shown in Fig. 2 as designed above is stable if

$$\left\| (sI - (A_m + K))^{-1} \cdot (BB^+(1 - G_f(s))\Delta A \right.$$
$$\left. - (I - BB^+)(A_m + K - A - \Delta A)) \right\|_\infty < 1. \quad (32)$$

Proof. The closed-loop system dynamics in (31) is

$$[I - (sI - (A_m + K))^{-1}(BB^+(1 - G_f(s))\Delta A$$
$$- (I - BB^+)(A_m + K - A - \Delta A))]X(s)$$
$$= (sI - (A_m + K))^{-1}(BB^+(B_m C(s)$$
$$- KX_m(s)) + (I - BB^+ G_f(s))D(s)).$$

Since the reference model, $(sI - (A_m + K))^{-1}$, and $G_f(s)$ are all designed to be stable, according to the small-gain theorem [32], the closed-loop system shown in Fig. 2 is stable if condition (32) is met. This completes the proof.

This theorem holds no matter the structural constraint (8) is satisfied or not. A special case is given below.

Corollary 2: Assume that the system shown in Fig. 2 satisfies $(I - BB^+)(A_m + K - A - \Delta A) = 0$. Then, the system is stable if

$$\left\| (sI - (A_m + K))^{-1} \cdot BB^+(1 - G_f(s))\Delta A \right\|_\infty < 1. \quad (33)$$

It is obvious after substituting $(I - BB^+)(A_m + K - A - \Delta A) = 0$ into (32).

Theorem 3: Assume that the closed-loop system shown in Fig. 2 as designed above satisfies the structural constraint (8). Then, the system is stable if

$$\left\| (sI - (A_m + K))^{-1} \cdot BB^+(1 - G_f(s))\Delta A \right\|_\infty < 1. \quad (34)$$

Proof. If the structural constraint (8) is satisfied, then the actual error dynamics given in (30) is reduced to

$$sE(s) = (A_m + K)E(s) - BB^+(1 - G_f(s))U_d(s)$$

which gives the following closed-loop system dynamics:

$$(sI - (A_m + K) - BB^+(1 - G_f(s))\Delta A)X(s)$$
$$= B_m C(s) - KX_m(s) + BB^+(1 - G_f(s))D(s). \quad (35)$$

Since the reference model, $(sI - (A_m + K))^{-1}$, and $G_f(s)$ are all designed to be stable, the system is stable if the condition (34) is met, according to the small-gain theorem.

These theorems provide some insights for choosing the design parameters in the UDE-based controller to guarantee the stability of the closed-loop system in different cases. The small-gain conditions (32)–(34) can be satisfied by increasing K or tuning the filter transfer function $G_f(s)$ close to 1 through the suitable selection of $N_d(s)$.

B. Asymptotic Performance

Even if the closed-loop system is stable, it does not necessarily guarantee asymptotic performance. The following sufficient condition does.

Theorem 4: The closed-loop system shown in Fig. 2 as designed above achieves asymptotic reference tracking and disturbance rejection if 1) the closed-loop system is stable and 2) the structural constraint (8) is met.

Proof. When the closed-loop system is stable, all signals in the closed loop are bounded. From Fig. 2, there must exist a stable transfer function from the reference $R(s)$ to the state $X(s)$, denoted as $G_{RX}(s)$ here for any reference. Therefore

$$U_d(s) = \Delta A X(s) + D(s) = \Delta A \cdot G_{RX}(s) R(s) + D(s).$$

Since the disturbance exosystem S_d and the reference exosystem S_r are included in the design of $G_f(s)$, we have

$$(1 - G_f(s))U_d(s) = \frac{lcm(|sI - S_r|, |sI - S_d|)}{N_d(s)}$$
$$\times \left(\Delta A G_{RX}(s) \frac{P_r}{|sI - S_r|} + \frac{P_d}{|sI - S_d|} \right). \quad (36)$$

Hence,

$$\lim_{s \to 0} s \cdot (1 - G_f(s))U_d(s) = 0 \quad (37)$$

which implies that the estimation error of the uncertainty and disturbance term $u_d(t)$ converges to zero eventually according to the final-value theorem, i.e.,

$$\lim_{t \to \infty} \tilde{u}_d(t) = \lim_{t \to \infty} (u_d(t) - \hat{u}_d(t)) = 0.$$

If the structural constraint (8) is met, then according to the general error dynamics (30), we have

$$E(s) = -(sI - (A_m + K))^{-1} BB^+ (1 - G_f(s))U_d(s). \quad (38)$$

Substituting (37) into the error dynamics (38) and applying the final-value theorem, we obtain

$$\lim_{t \to \infty} e(t) = \lim_{s \to 0} s \cdot E(s) = 0. \quad (39)$$

Hence, $x(t)$ asymptotically tracks the reference state $x_m(t)$. According to the designed transfer function from $R(s)$ to $X_{m1}(s)$ in (19), with the choice of $M_r(s)$ in (18) and the stabilizer $N_r(s)$, the internal model principle guarantees that $x_{m1}(t)$ asymptotically tracks $r(t)$. As a result, the output $y(t) = [1\ 0\ \cdots\ 0]_{1 \times n} \cdot x(t) = x_1(t)$, as in Fig. 2, asymptotically tracks the reference $r(t)$. In other words, asymptotic reference tracking and disturbance rejection are achieved.

C. Impact of Measurement Noise and Selection of $N_d(s)$

In Fig. 2, the closed-loop transfer function from $N(s)$ to $U(s)$ can be obtained as

$$H_{NU}(s) = \{1 - B^+[A_m - A + K - G_f(s)\Delta A]$$
$$\cdot [sI - (A + \Delta A)]^{-1} B\}^{-1}$$
$$\cdot B^+[A_m - A + K - sG_f(s)I + G_f(s)A].$$

In order to show the impact of the noise $N(s)$, a filter $G_f(s) = \frac{1}{\tau s + 1}$ is considered as an example. Since $G_f(s)$ is strictly stable, with $s \to \infty$, $G_f(s) \to 0$ and $sG_f(s) \to \frac{1}{\tau}$, which is the bandwidth of the filter. For high frequencies, the gain is

$$H_{NU}(\infty) = B^+ \left(A_m + K - A - \frac{1}{\tau}I \right). \quad (40)$$

If the bandwidth of the filter $G_f(s)$ is too wide, which means τ is small, then the high-frequency noise $N(s)$ will be amplified and the control signal will be polluted. Therefore, there exists a tradeoff about the choice of the bandwidth of $G_f(s)$ between the good estimation of the uncertainty and disturbance term and the mitigation of the high-frequency measurement noise. What is good is that, in practice, the measurement noise can be handled by adding a filter, either physically or digitally. Hence, the tradeoff is often not a problem.

According to (24)

$$G_f(s) = \frac{N_d(s) - M_d(s)}{N_d(s)}.$$

The selection of $N_d(s)$ should consider the following.
1) $G_f(s)$ is stable.
2) The bandwidth of $G_f(s)$ meets the tradeoff with the measurement noise.
3) $G_f(s)$ satisfies condition (34).

D. Structural Constraint

As mentioned in Section II-A, the structural constraint (8) determines if (7) is an accurate solution or a least-squares approximate solution of (5). Even if the structural constraint is not satisfied, the stability of the closed-loop system with the UDE-based control can still be achieved, but the asymptotic performance may not be guaranteed. This can be seen from (30), where there exists a term that cannot converge to 0. For the system (1) considered in this paper, if B is invertible, e.g., $n = 1$, the structural constraint is always met. Otherwise, the choices of the reference model and the error feedback gain matrix are somewhat restricted. For example, if the system (1) is realized in the controllable companion form, i.e., $A = \begin{bmatrix} 0 & I_{n-1} \\ & A_n \end{bmatrix}$, $B = \begin{bmatrix} 0 \\ b_n \end{bmatrix}$, where A_n is a row vector and b_n is a scalar, then $I - BB^+ = \begin{bmatrix} I_{n-1} & 0 \\ 0 & 0 \end{bmatrix}$. In order to satisfy the structural constraint (8), the uncertainty ΔA and disturbance d should meet the so-called matching condition, i.e., $\Delta A = \begin{bmatrix} 0 \\ \Delta A_n \end{bmatrix}$, $d = \begin{bmatrix} 0 \\ d_n \end{bmatrix}$, where ΔA_n is a row vector and d_n is a scalar. Furthermore, the selections of A_m, B_m, and K in the reference model are limited as $A_m = \begin{bmatrix} 0 & I_{n-1} \\ & A_{mn} \end{bmatrix}$, $B_m = \begin{bmatrix} 0 \\ b_{mn} \end{bmatrix}$, and $K = \begin{bmatrix} 0 \\ K_n \end{bmatrix}$, where A_{mn} is a row vector and b_{mn} and K_n are scalar. This indicates that the reference model is also in the controllable companion form, and the error feedback gain matrix K should meet the matching condition. With the above selections, the structural constraint (8) is satisfied, because $(I - BB^+)(A_m x(t) + B_m c(t) - Ax(t) - u_d - Ke(t)) = \begin{bmatrix} I_{n-1} & 0 \\ 0 & 0 \end{bmatrix} \begin{bmatrix} 0 \\ f \end{bmatrix} = 0$, where f is a nonzero value. The experimental platform to be conducted in next section belongs to this special case.

VI. EXPERIMENTAL STUDIES

In order to demonstrate the asymptotic tracking and disturbance rejection performance of the proposed UDE-based robust control, the experimental validation was carried out on a rotary servo system as an example. The system consists of a QUANSER rotary servo motor, a QUANSER single channel linear voltage amplifier, and a dSPACE 1104 device with a 12-bit A/D converter. The angular position resolution of this experimental setup is $0.17°$. The sampling time is 0.001 s.

The model of this servo system is described as

$$\begin{bmatrix} \dot{\theta} \\ \ddot{\theta} \end{bmatrix} = (A + \Delta A)\begin{bmatrix} \theta \\ \dot{\theta} \end{bmatrix} + Bu + d(t) \tag{41}$$

where θ and $\dot{\theta}$ are the states that represent the angular position and velocity, respectively, $A = \begin{bmatrix} 0 & 1 \\ 0 & -30 \end{bmatrix}$, ΔA is the unknown state matrix, $B = \begin{bmatrix} 0 & 80 \end{bmatrix}^T$, u is the control signal to be designed, and $d(t) = \begin{bmatrix} 0 & 80d_2(t) \end{bmatrix}^T$ with $d_2(t)$ as the external disturbance signal.

A. Case I: Performance With Different Filters

In this study, the step external disturbance $d_2(t) = 100$ is added at $t = 4$ s and the uncertainty $\Delta A = \begin{bmatrix} 0 & 0 \\ 0 & -20 \end{bmatrix}$ is added at $t = 8$ s. According to (6), the uncertainty and disturbance term $u_d = \Delta A\begin{bmatrix} \theta \\ \dot{\theta} \end{bmatrix} + d(t) = \begin{bmatrix} 0 \\ u_{d2} \end{bmatrix}$. The objective is to design the controller u to make the servo motor system (41) follow the desired trajectory $r(t) = 40\sin(2\pi t)$ degrees. The following stable second-order reference system is chosen:

$$\begin{bmatrix} \dot{\theta}_m \\ \ddot{\theta}_m \end{bmatrix} = \begin{bmatrix} 0 & 1 \\ -\omega^2 & -2\zeta\omega \end{bmatrix}\begin{bmatrix} \theta_m \\ \dot{\theta}_m \end{bmatrix} + \begin{bmatrix} 0 \\ \omega^2 \end{bmatrix}c(t) \tag{42}$$

where θ_m and $\dot{\theta}_m$ are the reference states, $c(t)$ is the command signal to the reference model, and ω and ζ are the reference model parameters, which are chosen as $\omega = 20\pi$ and $\xi = 0.3$ in this study. As discussed in Section III, the asymptotic reference tracking of $\theta_m(t) \to c(t)$ when $t \to \infty$ is not always guaranteed by (42) for the general type of command signal $c(t)$. Thus, the control strategy shown in Fig. 1 is adopted to achieve asymptotic tracking of the general type of command signal $r(t)$. According to the discussions in Section III, in order to achieve the asymptotic tracking of a sinusoidal reference signal, the internal model in Fig. 1 is set as $N_r(s) = 10\,s + 1$, $M_r(s) = s^2 + 4\pi^2$.

The error feedback gain matrix is chosen as $K = 0$. It is easy to validate that the structural constraint (8) is satisfied. The filter in the UDE-based control plays a very important role for the UDE and three filters G_{f1}, G_{f2}, and G_{f3} were derived for a step or sinusoidal type of disturbance rejection based on the internal model principle in Section IV. In this subsection, the comparison of these three filters is provided for the sinusoidal tracking and step disturbance rejection. To guarantee the uncertainty estimation accuracy, the bandwidth of filters should cover the maximum frequency of the disturbance signal. The cutoff frequency of the three filters G_{f1}, G_{f2}, and G_{f3} is set at around $200\,\pi$ rad/s. According to the internal model

TABLE I
FILTERS AND PARAMETERS

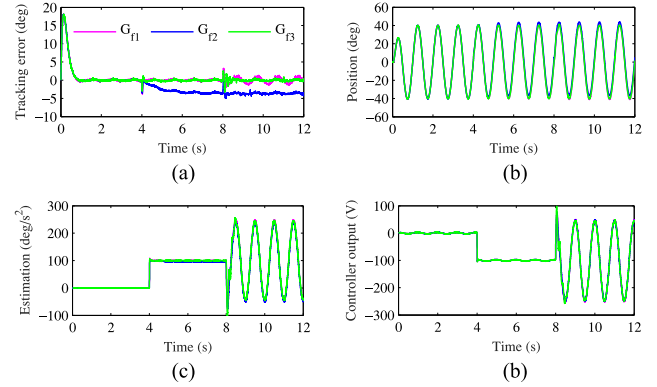|		a	a_1	a_2	ω_0
G_{f1}	$\dfrac{a}{s+a}$	200π	–	–	–
G_{f2}	$\dfrac{a_1 s + a_2 - \omega_0^2}{s^2 + a_1 s + a_2}$	–	$100\omega_0$	$100\omega_0^2$	2π
G_{f3}	$\dfrac{(a+a_1)s^2 + (a_2 + aa_1 - \omega_0^2)s + aa_2}{(s+a)(s^2 + a_1 s + a_2)}$	10π	$90\omega_0$	$10\omega_0^2$	2π

Fig. 3. Case I: Rejection of disturbance and uncertainty by using UDE with G_{f1}, G_{f2}, G_{f3}. (a) Position tracking error. (b) Position. (c) Uncertainty estimation. (d) Controller output.

TABLE II
STEADY-STATE TRACKING ERRORS (RMS, DEGREE) FOR CASE I

Period	UDE-based control		
	G_{f1}	G_{f2}	G_{f3}
2–4 s nominal	0.18	0.17	0.17
6–8 s step	0.18	3.48	0.18
10–12 s step+sin	0.76	3.61	0.19

principle, the design of $M_d(s)$ is determined by the disturbance exosystem and the reference exosystem, while $N_d(s)$ should be chosen for the given cutoff frequency and make sure the filter $G_f(s)$ satisfies the stability condition in Theorem 3. The parameters of three filters are summarized in Table I.

The experimental results using the UDE-based control with the three filters are shown in Fig. 3. The zero initial conditions are set for both the reference model and the system model. From Fig. 3(a), it can be seen that when $t < 4$ s, without system uncertainty and external disturbance (i.e., $\Delta A = 0$ and $d(t) = 0$), after some transient process, three controllers with different filters have comparable tracking performance and the tracking errors of three cases all converge to zero. As shown in Table II, all of the root mean square (RMS) steady-state tracking errors for G_{f1}, G_{f2}, and G_{f3} during 2–4 s are around $0.17°$, which has actually reached the hardware resolution limit. When the large step disturbance is added at $t = 4$ s with $d_2(t) = 100(t - 4)$, the estimated uncertainty and disturbance term $\hat{u}_{d2}/80$ is shown in Fig. 3(c), and a large spike occurs in the tracking errors, as

shown in Fig. 3(a). For $4 < t < 8$ s, the three controllers try to reject the step disturbance and follow the desired reference signal. There exists a nonzero steady-state error for the controller with G_{f2}, while asymptotic tracking can be achieved with G_{f1} and G_{f3}. This is due to the asymptotic disturbance rejection by including the step disturbance mode into the design of G_{f1} and G_{f3}, as discussed in Section IV, while G_{f2} fails to do so. Table II shows the RMS steady-state tracking error for G_{f2} during 6–8 s is as large as $3.48°$, while for the other two, it still remains at $0.18°$. At $t = 8$ s, the system uncertainty $\Delta A = \begin{bmatrix} 0 & 0 \\ 0 & -20 \end{bmatrix}$ is added to the system, which results in a large mixed sinusoidal and step signal in the uncertainty and disturbance term u_d in (6), as shown in Fig. 3(c). and another spike occurred at $t = 8$ s in the tracking errors in Fig. 3(a). When $t > 8$ s, the tracking performance of the controller with G_{f3} is superior to the other cases, as both the sinusoidal and step modes are included in the design of G_{f3}. Indeed, the RMS steady-state tracking errors for G_{f1}, G_{f2}, and G_{f3} during 10–12 s in Fig. 3(a) are $0.76°$, $3.61°$, and $0.19°$, respectively, as shown in Table II. It is worth highlighting that the RMS tracking error for G_{f3} has almost reached the hardware resolution limit of $0.17°$, the best achievable performance. The estimation of the lumped uncertainty and disturbance ($\hat{u}_{d2}/80$) and the controller signal u are plotted in Fig. 3(c) and (d), respectively. Note that the small-gain condition (34) of G_{f1} and G_{f3} is satisfied (calculated as 0.030 and 0.033, respectively). Though G_{f2} does not satisfy this condition, the controller still works well, because the condition is only sufficient.

B. Case II: Rejection of an Unknown Disturbance Having two Frequency Components and White Noises

In practice, disturbances can have different types and frequency components, which can be identified by Fourier analysis. Once the major frequencies are identified, the filter can be designed. In this subsection, the case with an unknown disturbance is investigated, with the only preliminary information that the major frequency components are around 2π and 6π rad/s. The exact frequency, phase, and amplitude of the individual frequency components of the disturbance are not known for the design. In order to make it more practical, the disturbance is assumed to have been polluted by white noises. According to the preliminary frequency information of the disturbance, a new filter

$$G_{f4}(s) = 1 - \frac{(s^2 + 4\pi^2)(s^2 + 36\pi^2)}{(s^2 + 200\pi s + 40\pi^2)(s^2 + 3\pi s + 36\pi^2)}$$

is designed to achieve the bandwidth around 200π rad/s.

Experiments were carried out with $G_{f4}(s)$. The randomly chosen unknown disturbance, as shown in Fig. 4(c), is $d_2(t) = 13.2\sin(1.7\pi t + \frac{\pi}{3}) + 35.7\sin(4.3\pi t - \frac{\pi}{6}) + n$, where n is the white noise with noise power of 2 and sample time of 0.05 s. The lower frequency component of $d_2(t)$ is applied at $t = 4$ s and the higher frequency disturbance of $d_2(t)$ is applied at $t = 8$ s, which means, after 8 s, the disturbance has two unknown frequency components. The white noise is applied during the whole experiment. As shown in Fig. 4, the UDE-based controller can
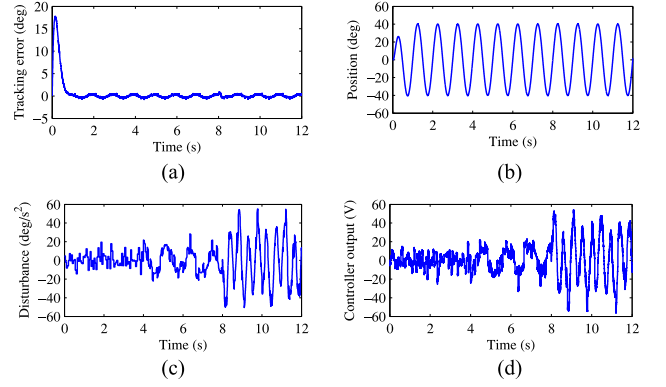

Fig. 4. Case II: Rejection of an unknown disturbance polluted with white noises by using the UDE with G_{f4}. (a) Position tracking error. (b) Position. (c) Disturbance. (d) Controller output.

still cope with the very practical disturbance. The RMS steady-state tracking errors are $0.20°$, $0.19°$, and $0.21°$, respectively, for the three time intervals. The errors are slightly bigger than those in Case I with G_{f3} but still very close to the hardware resolution. Fig. 4(d) illustrates the control signal u, which clearly cancels the unknown disturbance $d_2(t)$ shown in Fig. 4(c) well.

C. Case III: Comparison With Other Robust Controllers

In order to demonstrate the advantages of the proposed UDE-based control, comparative studies with the DOB-based control and the ADRC are carried out. Because of the noisy control signals of DOB and ADRC, which will be shown in detail later, the amplitudes of the desired trajectory, the disturbance, and the uncertainty have to be reduced dramatically. Otherwise, the control signals would saturate, leading to instability. The desired trajectory is changed to $r(t) = 30\sin(2\pi t)$ degrees; the external disturbance added at $t = 4$ s is reduced to $d_2(t) = 10$; and the system uncertainty added at $t = 8$ s is reduced to $\Delta A = \begin{bmatrix} 0 & 0 \\ 0 & -2 \end{bmatrix}$. The UDE-based control with G_{f3} designed in Section VI-A is adopted for comparison with the experimental results shown in the left column of Fig. 5. As shown in Table III, the RMS steady-state tracking error of UDE with G_{f3} is $0.18°$ during 2–4 s, $0.18°$ during 6–8 s, and $0.19°$ during 10–12 s, which is very close to what is achieved in Section VI-A. As a byproduct, this has demonstrated that the robust performance of UDE-based control is very consistent under different scenarios.

1) Comparison With Internal-Model-Embedded DOB: The internal-model-embedded DOB [33] is considered for comparison. The nominal transfer function of the system can be written as $G_n(s) = \frac{80}{s^2 + 30s}$; then, its inverse is $G_n^{-1}(s) = \frac{s^2 + 30s}{80}$. For fair comparison, the outer-loop controller is chosen as $u_c(t) = [-\omega_d^2(x_1 - x_{1r}) - 2\zeta_d\omega_d(x_2 - \dot{x}_{1r}) + \ddot{x}_{1r} + 30x_2]/80$, with $\omega_d = 20\pi$ and $\xi_d = 0.3$. The filter of DOB is chosen as $Q(s) = \frac{\{6 - (\tau\omega_0)^2\}(\tau s)^2 + \{3.8 - 4(\tau\omega_0)^2\}(\tau s) + 0.04}{(\tau s)^4 + 4(\tau s)^3 + 6(\tau s)^2 + 3.8(\tau s) + 0.04}$, with $\tau = 0.008$ chosen to achieve the best possible performance. The experimental results are shown in the middle column of Fig. 5 with the steady-state performance summarized in Table III. As can be seen, the RMS steady-state tracking
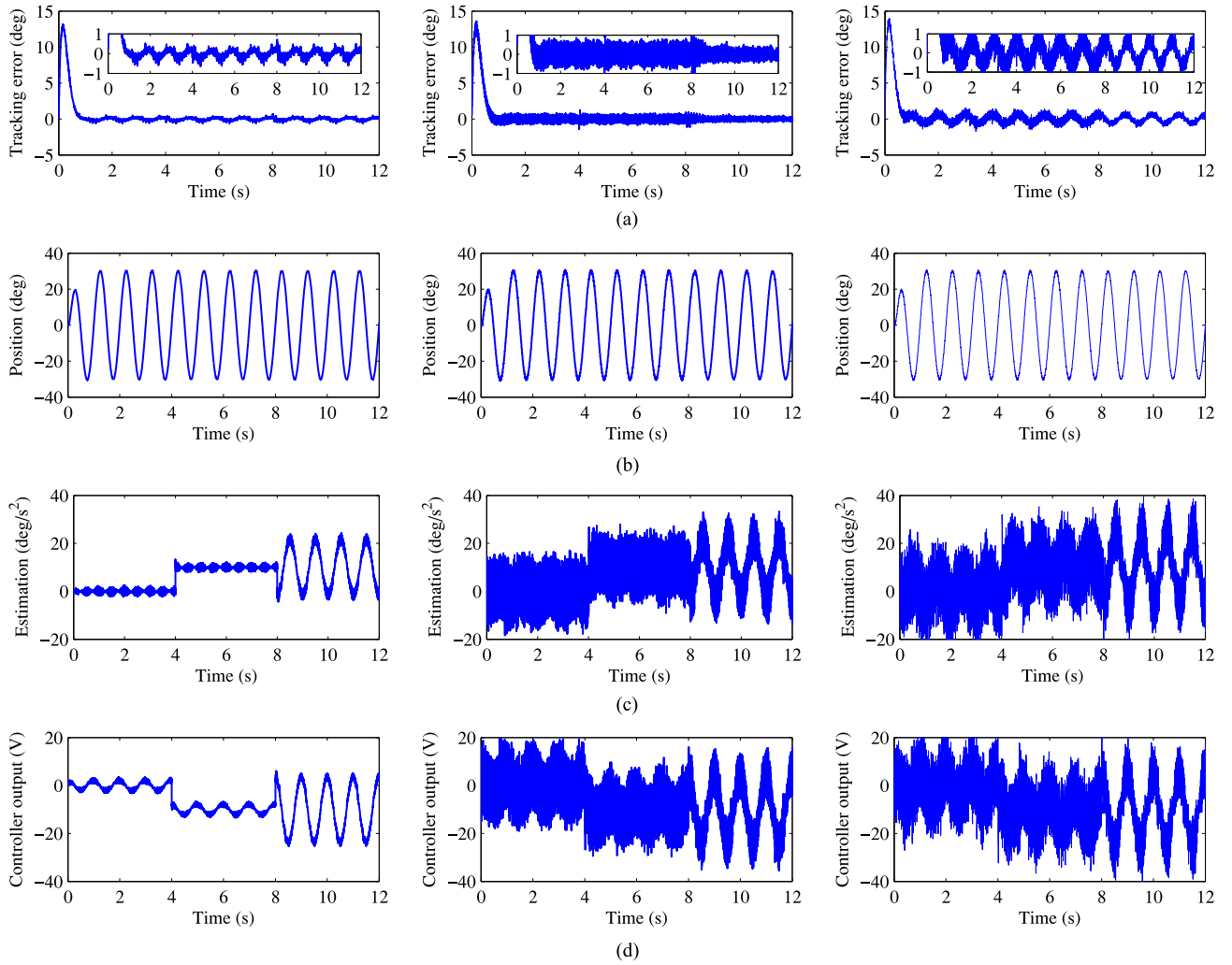
Fig. 5. Case III: Comparisons: UDE with G_{f3} (left); internal-model-embedded DOB [33] (middle); third-order ADRC [34] (right). (a) Position tracking error. (b) Position. (c) Uncertainty estimation. (d) Controller output.

TABLE III
STEADY-STATE TRACKING ERRORS (RMS, DEGREE) AND CONTROL
EFFORTS (RMS, V) FOR CASE III

		UDE	DOB	ADRC
2–4 s nominal	$e(t)$	0.18	0.37	0.57
	$u(t)$	1.57	8.12	11.75
6–8 s step	$e(t)$	0.18	0.37	0.56
	$u(t)$	10.11	12.73	15.49
10–12 s step+sin	$e(t)$	0.19	0.19	0.46
	$u(t)$	14.02	14.69	16.46

errors from the DOB are $0.37°$ during 2–4 s, $0.37°$ during 6–8 s, and $0.19°$ during 10–12 s, respectively. The best tracking performance of the internal-model-embedded DOB, during 10–12 s, is quite close to that of the UDE-based control. However, as shown in Fig. 5(d), the DOB-based control suffers from serious high-frequency spikes in the control signal, due to the derivative term in the outer-loop controller. Indeed, decreasing the outer-loop controller gain could reduce the spikes in the control signal,

but this would increase the tracking error because of the trade-off of the DOB control between the tracking performance and the noise amplification in the control signal. The total harmonic distortion of the control signal during 10–12 s is 44%, while it is 5% for the control signal from the UDE-based control. In addition, the DOB also requires a larger control effort compared to the UDE, as shown in Table III.

2) Comparison With Third-Order ADRC: ADRC is another popular robust control method [35], [36]. Its basic idea is that the system uncertainties and disturbance term can be regarded as an extended state and estimated by an ESO. In this case, the servo system (41) can be rewritten as

$$\dot{x}_1 = x_2$$
$$\dot{x}_2 = x_3 + 80u$$
$$\dot{x}_3 = x_4 \qquad\qquad (43)$$
$$\dot{x}_4 = x_5$$
$$\dot{x}_5 = \ddot{h}$$

where $x_1 = \theta$, $x_2 = \dot{\theta}$, the extended state $x_3 = \Delta + d$, which is the total uncertainty and disturbance term, $x_4 = \dot{x}_3$ and $x_5 = \ddot{x}_3$ are the derivatives of the total disturbance, and $h = \dot{x}_3$ is an unknown function. In order to improve the performance, a third-order ESO is designed by following [34] and [36] as

$$
\begin{aligned}
\dot{z}_1 &= z_2 + 5\omega_{rc}(x_1 - z_1) \\
\dot{z}_2 &= z_3 + 10\omega_{rc}^2(x_1 - z_1) + 80u \\
\dot{z}_3 &= z_4 + 10\omega_{rc}^3(x_1 - z_1) \\
\dot{z}_4 &= z_5 + 5\omega_{rc}^4(x_1 - z_1) \\
\dot{z}_5 &= \omega_{rc}^5(x_1 - z_1)
\end{aligned}
\tag{44}
$$

where z_1, z_2, z_3, z_4, and z_5 are the estimations of system states, and ω_{rc} is the bandwidth of the ESO, which is chosen as $\omega_{rc} = 80\,\pi$ rad/s. The nonlinear controller is designed as $u = [\ddot{x}_{1r} - \omega_a^2(x_1 - x_{1r}) - 2\omega_a(x_2 - \dot{x}_{1r}) - z_3]/80$, with the controller bandwidth of $\omega_a = 18\,\pi$ rad/s. The experimental results are shown in the right column of Fig. 5, with the steady-state performance summarized in Table III. The RMS steady-state tracking errors from the ADRC are $0.57°$, during 2–4 s, $0.56°$ during 6–8 s, and $0.46°$ during 10–12 s, respectively. Increasing the bandwidth of the ESO could decrease the tracking error, and theoretically, the asymptotic convergence could be guaranteed when ω_{rc} goes to ∞ [37]. However, this is limited in practice for various reasons. Moreover, the third-order ADRC is also sensitive to the measurement noise and suffers from serious spikes in the control signal, as shown in Fig. 5(d). The total harmonic distortion of the control signal during 10–12 s is 71%, while it is 5% for the UDE-based control. Its control effort is also much greater than that of the UDE, as shown in Table III.

VII. Conclusion

In this paper, a systematic approach was proposed to achieve asymptotic reference tracking and disturbance rejection for the UDE-based robust control strategy. By applying the internal model principle, the information of the exosystems to generate all the desired trajectory and disturbances was incorporated into the reference system design and the filter design of UDE-based control. Moreover, the conditions to guarantee the closed-loop system stability and to achieve asymptotic disturbance rejection and reference tracking were derived. Experimental results have demonstrated excellent overall performance, with comparison to the internal-model-embedded DOB-based control and a third-order ADRC. The advantage of the proposed method lies in its capability of estimating system uncertainties and disturbances to push the performance to the hardware resolution limit, at the cost of a relatively fast sampling rate. However, a fast sampling rate is no longer a major issue for many applications nowadays because modern microcontrollers can easily be operated with a sampling rate at kilohertz or tens of kilohertz. The proposed method requires the range of the dominant frequency components of the disturbance, which can be identified by Fourier analysis in most practical cases. How to achieve excellent performance without this information and extend the method to nonlinear systems should be further investigated. The method in this paper may also shed some lights on improving other controllers too.

References

[1] M. Krstić, I. Kanellakopoulos, and P. V. Kokotović, *Nonlinear and Adaptive Control Design*. New York, NY, USA: Wiley, 1995.

[2] S. S. Ge, C. C. Hang, T. H. Lee, and T. Zhang, *Stable Adaptive Neural Network Control*. Boston, MA, USA: Kluwer, 2002.

[3] F. L. Lewis, S. Jagannathan, and A. Yesilidrek, *Neural Network Control of Robot Manipulators and Nonlinear Systems*. Philadelphia, PA, USA: Taylor & Francis, 1999.

[4] X. Li and C. C. Cheah, "Adaptive neural network control of robot based on a unified objective bound," *IEEE Trans. Control Syst. Technol.*, vol. 22, no. 3, pp. 1032–1043, May 2014.

[5] K. Zhou, J. C. Doyle, and K. Glover, *Robust and Optimal Control*. Upper Saddle River, NJ, USA: Prentice-Hall, 1996.

[6] V. I. Utkin, *Sliding Modes and their Application in Variable Structure Systems*. Moscow, Russia: MIR, 1978.

[7] X.-G. Yan, S. K. Spurgeon, and C. Edwards, "Memoryless static output feedback sliding mode control for nonlinear systems with delayed disturbances," *IEEE Trans. Autom. Control*, vol. 59, no. 7, pp. 1906–1912, Jul. 2014.

[8] S. Ding, J. Wang, and W. X. Zheng, "Second-order sliding mode control for nonlinear uncertain systems bounded by positive functions," *IEEE Trans. Ind. Electron.*, vol. 62, no. 9, pp. 5847–5909, Sep. 2015.

[9] K. Ohishi, M. Nakao, K. Ohnishi, and K. Miyachi, "Microprocessor-controlled DC motor for load-insensitive position servo system," *IEEE Trans. Ind. Electron.*, vol. IE-34, no. 1, pp. 44–49, Feb. 1987.

[10] W.-H. Chen, D. J. Ballance, P. J. Gawthrop, J. J. Gribble, and J. O'Reilly, "A nonlinear disturbance observer for two-link robotic manipulators," *IEEE Trans. Ind. Electron.*, vol. 47, no. 4, pp. 932–938, Aug. 2000.

[11] Y. Choi, K. Yang, W. K. Chung, H. R. Kim, and I. H. Suh, "On the robustness and performance of disturbance observers for second-order systems," *IEEE Trans. Autom. Control*, vol. 48, no. 2, pp. 1–6, Feb. 2003.

[12] W.-H. Chen, J. Yang, L. Guo, and S. Li, "Disturbance-observer-based control and related methods: An overview," *IEEE Trans. Ind. Electron.*, vol. 63, no. 2, pp. 1083–1095, Feb. 2016.

[13] E. Sariyildiz and K. Ohnishi, "A guide to design disturbance observer," *J. Dyn. Syst., Meas. Control*, vol. 136, no. 2, Dec. 2014, Art. no. 021011.

[14] J. Han, "From PID to active disturbance rejection control," *IEEE Trans. Ind. Electron.*, vol. 56, no. 3, pp. 900–906, Mar. 2009.

[15] Z. Gao, "On the centrality of disturbance rejection in automatic control," *ISA Trans.*, vol. 53, no. 4, pp. 850–857, Jul. 2013.

[16] J. Yao, Z. Jiao, and D. Ma, "Adaptive robust control of DC motors with extended state observer," *IEEE Trans. Ind. Electron.*, vol. 61, no. 7, pp. 3630–3637, Jul. 2014.

[17] S. Li, J. Li, and Y. Mo, "Piezoelectric multimode vibration control for stiffened plate using ADRC-based acceleration compensation," *IEEE Trans. Ind. Electron.*, vol. 61, no. 12, pp. 6892–6902, Dec. 2014.

[18] W. Xue, W. Bai, S. Yang, K. Song, Y. Huang, and H. Xie, "ADRC with adaptive extended state observer and its application to air-fuel ratio control in gasoline engines," *IEEE Trans. Ind. Electron.*, vol. 62, no. 9, pp. 5899–5857, Sep. 2015.

[19] J. She, X. Xin, and Y. Pan, "Equivalent-input-disturbance approach—Analysis and application to disturbance rejection in dual-stage feed drive control system," *IEEE/ASME Trans. Mechatronics*, vol. 16, no. 2, pp. 330–340, Apr. 2011.

[20] K. Youcef-Toumi and O. Ito, "A time delay controller for systems with unknown dynamics," *J. Dyn. Syst., Meas. Control*, vol. 112, no. 1, pp. 133–142, Mar. 1990.

[21] Q.-C. Zhong and D. Rees, "Control of uncertain LTI systems based on an uncertainty and disturbance estimator," *J. Dyn. Syst., Meas. Control Trans.*, vol. 126, no. 4, pp. 905–910, Dec. 2004.

[22] Q.-C. Zhong, A. Kuperman, and R. Stobart, "Design of UDE-based controllers from their two-degree-of-freedom nature," *Int. J. Robust Nonlinear Control*, vol. 21, pp. 1994–2008, Nov. 2011.

[23] B. Ren, Q.-C. Zhong, and J. Chen, "Robust control for a class of non-affine nonlinear systems based on the uncertainty and disturbance estimator," *IEEE Trans. Ind. Electron.*, vol. 62, no. 9, pp. 5881–5888, Sep. 2015.

[24] S. Talole and S. Phadke, "Robust input-output linearisation using uncertainty and disturbance estimation," *Int. J. Control*, vol. 82, no. 10, pp. 1794–1803, Aug. 2010.

[25] S. Talole, T. Chandar, and J. P. Kolhe, "Design and experimental validation of UDE based controller–observer structure for robust input–output linearisation," *Int. J. Control*, vol. 84, no. 5, pp. 969–984, Jun. 2011.

[26] T. S. Chandar and S. E. Talole, "Improving the performance of UDE-based controller using a new filter design," *Nonlinear Dyn.*, vol. 77, pp. 753–768, Aug. 2014.

[27] V. Deshpande and S. Phadke, "Control of uncertain nonlinear systems using an uncertainty and disturbance estimator," *J. Dyn. Syst., Meas. Control*, vol. 134, no. 2, Dec. 2012, Art. no. 024501.

[28] B. A. Francis and W. M. Wonham, "The internal model principle of control theory," *Automatica*, vol. 12, no. 5, pp. 457–465, Sep. 1976.

[29] J. Trumpf, H. L. Trentelman, and J. C. Willems, "Internal model principles for observers," *IEEE Trans. Autom. Control*, vol. 59, no. 7, pp. 1737–1749, Jul. 2014.

[30] R. Marino and P. Tomei, "Robust adaptive compensation of periodic disturbances with unknown frequency," *IEEE Trans. Autom. Control*, vol. 59, no. 10, pp. 2760–2765, Oct. 2014.

[31] L. Paunonen, "Designing controllers with reduced order internal models," *IEEE Trans. Autom. Control*, vol. 60, no. 3, pp. 775–780, Mar. 2015.

[32] H. K. Khalil, *Nonlinear Systems*. Englewood Cliffs, NJ, USA: Prentice-Hall, 2001.

[33] Y. Joo, G. Park, J. Back, and H. Shim, "Embedding internal model in disturbance observer with robust stability," *IEEE Trans. Autom. Control*, vol. 61, no. 10, pp. 3128–3133, Oct. 2016.

[34] A. A. Godbole, J. P. Kolhe, and S. E. Talole, "Performance analysis of generalized extended state observer in tackling sinusoidal disturbances," *IEEE Trans. Control Syst. Technol.*, vol. 21, no. 6, pp. 2212–2223, Nov. 2013.

[35] Z. Gao, "Scaling and bandwidth-parameterization based controller tuning," in *Proc. Amer. Control Conf.*, vol. 6, Jun. 2006, pp. 4989–4996.

[36] Q. Zheng and Z. Gao, "Predictive active disturbance rejection control for processes with time delay," *ISA Trans.*, vol. 53, no. 4, pp. 873–881, Jul. 2014.

[37] B.-Z. Guo and Z.-L. Zhao, "On the convergence of an extended state observer for nonlinear systems with uncertainty," *Syst. Control Lett.*, vol. 60, no. 6, pp. 420–430, Jun. 2011.

Qing-Chang Zhong (M'04–SM'04–F'17) received the Ph.D. degree in control theory and engineering from Shanghai Jiao Tong University, Shanghai, China, in 2000, and the Ph.D. degree in control and power engineering from Imperial College London, London, U.K., in 2004.

He is the Max McGraw Endowed Chair Professor in Energy and Power Engineering in the Department of Electrical and Computer Engineering, Illinois Institute of Technology, Chicago, IL, USA. He (co-)authored three research monographs: *Control of Power Inverters in Renewable Energy and Smart Grid Integration* (Wiley-IEEE Press, 2013), *Robust Control of Time-Delay Systems* (Springer-Verlag, 2006), *Control of Integral Processes with Dead Time* (Springer-Verlag, 2010), and a fourth, *Power Electronics-enabled Autonomous Power Systems: Next Generation Smart Grids*, is scheduled for publication by Wiley-IEEE Press. He proposed the architecture for the next-generation smart grids based on the synchronization mechanism of synchronous machines to unify the interface and interaction of power system players with the grid and achieve autonomous operation of power systems. His research focuses on power electronics, advanced control theory and the seamless integration of both to address fundamental challenges in energy and power systems.

Dr. Zhong is a Fellow of the Institution of Engineering and Technology, U.K., the Vice-Chair of the IFAC Technical Committee on Power and Energy Systems, and was a Senior Research Fellow of the Royal Academy of Engineering/Leverhulme Trust, U.K. (2009–2010) and the U.K. Representative to the European Control Association (2013–2015). He is an Associate Editor for the IEEE TRANSACTIONS ON AUTOMATIC CONTROL, IEEE TRANSACTIONS ON POWER ELECTRONICS, IEEE TRANSACTIONS ON INDUSTRIAL ELECTRONICS, IEEE TRANSACTIONS ON CONTROL SYSTEMS TECHNOLOGY, IEEE ACCESS, and IEEE JOURNAL OF EMERGING AND SELECTED TOPICS IN POWER ELECTRONICS. He is a Distinguished Lecturer of the IEEE Power Electronics Society, IEEE Control Systems Society, and IEEE Power and Energy Society.

Beibei Ren (S'05–M'10) received the B.Eng. degree in mechanical and electronic engineering and the M.Eng. degree in automation from Xidian University, Xi'an, China, in 2001 and 2004, respectively, and the Ph.D. degree in electrical and computer engineering from the National University of Singapore, Singapore, in 2010.
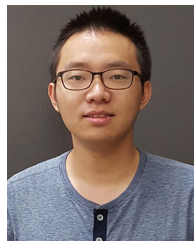
From 2010 to 2013, she was a Postdoctoral Scholar in the Department of Mechanical and Aerospace Engineering, University of California, San Diego, CA, USA. Since 2013, she has been with the Department of Mechanical Engineering, Texas Tech University, Lubbock, TX, USA, as an Assistant Professor. Her current research interests include robust control theory and its application in renewable energy systems, integration of renewables with grid, and unmanned aerial vehicles.

Jiguo Dai (S'15) received the B.Eng. degree in thermal energy and power engineering from Northwestern Polytechnical University, Xi'an, China, in 2013. He is currently working toward the Ph.D. degree in the Department of Mechanical Engineering, Texas Tech University, Lubbock, TX, USA.

His current research interests include robust control theory and its applications.